

The Indices of Refraction of Molecular-Beam Epitaxy-Grown $\text{Be}_x\text{Zn}_{1-x}\text{Te}$ Ternary Alloys

F.C. PEIRIS,^{1,3} M.R. BUCKLEY,¹ O. MAKSIMOV,² M. MUNOZ,²
and M.C. TAMARGO²

1.—Department of Physics, Kenyon College, Gambier, OH 43022. 2.—Department of Chemistry, City College and Graduate Center, CUNY, New York, NY 10031. 3.—E-mail: peirisf@kenyon.edu

We have used a combination of prism-coupling, reflectivity, and ellipsometric techniques to investigate the indices of refraction, n , of a series of $\text{Be}_x\text{Zn}_{1-x}\text{Te}$ thin films grown on InP substrates. After determining the concentrations of each of the $\text{Be}_x\text{Zn}_{1-x}\text{Te}$ alloys using x-ray diffraction measurements, we measured their n at discrete wavelengths using a prism-coupler setup. In addition, we used reflectivity measurements to complement the prism-coupler data and arrive at the dispersion relations of n for the $\text{Be}_x\text{Zn}_{1-x}\text{Te}$ alloys below their fundamental energy gaps. We then employed a rotating analyzer-spectroscopic ellipsometer to measure the complex reflection ratio for each of the films at angles of incidence of 65° , 70° , and 75° . By using the n values obtained from both the prism-coupler and the reflection-spectroscopy techniques to guide the ellipsometric analysis, we were able to obtain accurate results for the dispersion of n for the $\text{Be}_x\text{Zn}_{1-x}\text{Te}$ alloys, not only below their fundamental energy gaps, but also above their energy gaps (up to 6.5 eV) using these three complementary techniques.

Key words: $\text{Be}_x\text{Zn}_{1-x}\text{Te}$, molecular-beam epitaxy (MBE), index of refraction, prism coupler, reflectivity, ellipsometry

INTRODUCTION

It has been shown recently that beryllium-based II-VI semiconductor alloys form high-degree covalent bonds that result in lower defect densities and, consequently, increase the lifetimes associated with optoelectronic devices.¹ Due largely to these advantages, $\text{Be}_x\text{Zn}_{1-x}\text{Te}$ alloys have been recently proposed for applications in lasers and light-emitting diodes that operate in the visible wavelength range.^{2,3} In addition to its application benefits, there is also a theoretical interest in studying the $\text{Be}_x\text{Zn}_{1-x}\text{Te}$ ternary-alloy system because it undergoes a transition from a direct-gap material to an indirect-gap material at $x = 0.28$.⁴ If these alloys are to be used to fabricate novel optical devices, their optical properties must be well understood. Although there are a few studies reported on the bandgap and the excitonic properties of $\text{Be}_x\text{Zn}_{1-x}\text{Te}$, very little knowledge of the dispersion of the index of refraction, n , is presently available.

Although there are numerous experimental methods available to determine the n of thin films, such as interferometry, reflection spectroscopy, ellipsometry, and prism coupler, all of these techniques seem to suffer from deficiencies associated with their respective measuring technique or their analysis procedure. For instance, in both interferometry and reflection spectroscopy, one needs the prior knowledge of the film thickness to obtain accurate values for n .⁵ Although in the prism-coupler technique one is able to determine both n and the thickness, this method is limited by its inability to obtain n as a function of wavelength.⁶ This is because, due to experimental constraints, the prism-coupler method is most conveniently performed with a laser source, as opposed to a continuous source. Similarly, although it is possible to obtain the dispersion of n and the thickness from ellipsometric data, because of the large number of unknown parameters, this method can be nontrivial.⁷ Because each of these techniques by itself has inherent problems (as well as strengths), to obtain accurate values for the dispersion of n , one needs to implement a couple of these techniques concurrently.

(Received October 20, 2002; accepted November 13, 2002)

In this article, we have combined the prism-coupler, reflection-spectroscopy, and ellipsometry methods to obtain the dispersion of n for a series of $\text{Be}_x\text{Zn}_{1-x}\text{Te}$ alloys. Initially, we used the prism-coupler technique to find discrete values of n as well as the thickness of the semiconductor film. These parameters were then used to decipher the spectra obtained from reflection spectroscopy and to obtain the dispersion of n below the fundamental energy gap for the $\text{Be}_x\text{Zn}_{1-x}\text{Te}$ alloys. Because the ellipsometric spectra have to be carefully analyzed using several parameters to infer n , the prior knowledge of the thickness and the dispersion of n (below the fundamental gap) obtained from the prism-coupler and reflectivity methods facilitate this analysis. Hence, the results obtained, from both the prism coupler and the reflection spectroscopy, were used to guide the analysis of the ellipsometric spectra. By using these three experimental methods in unison, one is able to determine the dispersion of the n for $\text{Be}_x\text{Zn}_{1-x}\text{Te}$ alloys very accurately.

MOLECULAR-BEAM EPITAXY GROWTH AND STRUCTURAL CHARACTERIZATION

All of the thin $\text{Be}_x\text{Zn}_{1-x}\text{Te}$ films were grown by molecular-beam epitaxy (MBE) on semi-insulating, epi-ready (001) InP substrates using a Riber 2300 MBE system. Before depositing the $\text{Be}_x\text{Zn}_{1-x}\text{Te}$ films, the substrates were deoxidized at 500°C under As flux, and a $\sim 100\text{-nm}$ -thick, lattice-matched InGaAs-buffer layer was grown on the InP substrate. The growth temperature for the $\text{Be}_x\text{Zn}_{1-x}\text{Te}$ layer was maintained around 270°C . The growth rate was approximately $0.5 \mu\text{m/h}$, and $\text{Be}_x\text{Zn}_{1-x}\text{Te}$ layers were $0.5\text{--}1.5 \mu\text{m}$ thick. No cap layer was necessary, as no surface degradation of this material has been observed even over extended periods of time. We have used five samples of $\text{Be}_x\text{Zn}_{1-x}\text{Te}$ alloys for this study, with Be concentrations (x) ranging from $x = 0$ to $x = 0.378$.

The composition of the films was determined by using θ - 2θ x-ray diffraction experiments, assuming a linear dependence of the lattice constant with respect to the alloy concentration. In all of the x-ray diffraction spectra, the (004) reflection for $\text{Be}_x\text{Zn}_{1-x}\text{Te}$ is indicated by a single peak. Furthermore, a full-width at half-maximum in the range of $70\text{--}90$ arcsec was observed for the epilayers closely lattice matched to InP. The photoluminescence experiments performed at 6 K for these samples are dominated by narrow band-edge emission lines that indicate the high crystalline quality of the $\text{Be}_x\text{Zn}_{1-x}\text{Te}$ specimens.⁸

PRISM-COUPLER MEASUREMENTS

In the prism-coupler technique, a laser beam is coupled via a prism to the semiconductor layer for which n is of interest. The evanescent coupling between the prism and the semiconductor layer excites guided-wave modes in the layer, which depend on both n and on the thickness of the layer.⁹ Hence, both these

quantities can be determined if the semiconductor layer is sufficiently thick (i.e., if it can accommodate at least two guided modes within the layer). Using the prism-coupler technique, one can determine n with a precision of at least 0.1% and obtain the film thickness with an uncertainty of less than 0.5%.

The instrument was operated at two different wavelengths, and the measurements were made in transverse electric (TE) polarization mode. A He-Ne laser operating at 632.8 nm was used in conjunction with a rutile prism for one of the measurements, while a semiconductor-diode laser operating at 1300 nm was used with a Si prism for the other measurement. The experimental details concerning the prism-coupler method are discussed in Ref. 6. In Fig. 1, we show a rotation spectra obtained for one of the samples ($\text{Zn}_{0.831}\text{Be}_{0.169}\text{Te}$) at two different wavelengths. The dips in the reflected spectra shown in Fig. 1 correspond to the excitations of specific modes in the film. Both n and the thickness are calculated from the angular positions at which these dips occur in the reflected spectra. The n values obtained at the two discrete wavelengths as well as the thickness obtained for the film will be later used as input parameters to analyze the reflectivity and ellipsometric data.

It has to be mentioned that the n of the prism used in the experimental setup dictates the range of the n of the films that can be measured using the prism-coupler technique. For this reason, it is advantageous to use a prism that has an n that exceeds the n of the film. However, even in the absence of such prisms, the prism coupler is capable of determining the n and the thickness of films. Because the n of the $\text{Be}_x\text{Zn}_{1-x}\text{Te}$ alloys are greater than the value for n of rutile at 632.8 nm , as shown in Fig. 1b, the first few waveguide modes are absent from the spectra.¹⁰ Alternatively, as shown in Fig. 1a, because the n of the Si prism is greater than the n of the $\text{Be}_x\text{Zn}_{1-x}\text{Te}$ alloys, the spectra show the initial waveguide modes. When determining the n and the thickness from spectra

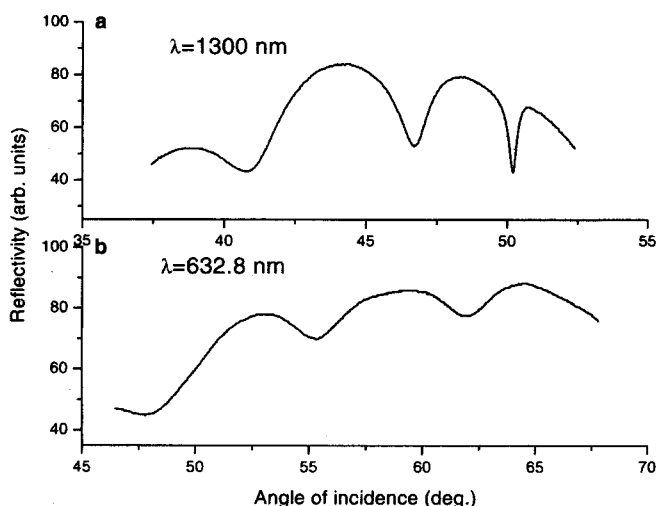


Fig. 1. A prism-coupler reflection spectrum obtained for $\text{Zn}_{0.831}\text{Be}_{0.169}\text{Te}$ at (a) $\lambda = 1,300 \text{ nm}$ and (b) $\lambda = 632.8 \text{ nm}$. The dips in the spectra correspond to the excitations of specific modes in the film.

such as Fig. 1b, one has to calculate these parameters together with their standard deviation, assuming that a specific number of modes are absent from the spectra. Following this procedure, the number of absent modes is found when the standard deviation for both n and the thickness are at their lowest values.

REFLECTION SPECTROSCOPY

The reflectivity technique is a complementary method suitable for determining the dispersion of n by carefully analyzing the Fabry-Perot oscillations in the reflection spectrum. However, to accurately determine the values for n from reflectivity measurements, one requires prior knowledge of the thickness of the film. This can usually be accomplished by another measurement, such as scanning electron microscopy. Because the prism-coupler method determines the thickness of semiconductor films with much higher accuracy than scanning electron microscopy, reflectivity data can be analyzed more accurately if they are combined with the prism-coupler data. Additionally, to correctly decipher the reflectivity spectra, one needs to determine the optical thickness corresponding to each of the extrema in the spectrum. Here again, one can use the discrete values of n determined by the prism-coupler method to obtain the optical thickness at the corresponding points in the reflectivity spectra.¹¹ With this input from the prism-coupler data, the reflectivity can produce a nearly continuous spectrum of n (usually, but not necessarily, obtained from positions of the Fabry-Perot maxima and minima).

The reflectivity measurements were carried out at normal incidence, and the data were calibrated using a Si-reference sample of known reflectivity. A typical spectrum is shown in Fig. 2 for the same sample as that used to illustrate the prism-coupler spectrum in Fig. 1. The Fabry-Perot oscillations seen in the spectrum arise from interference between

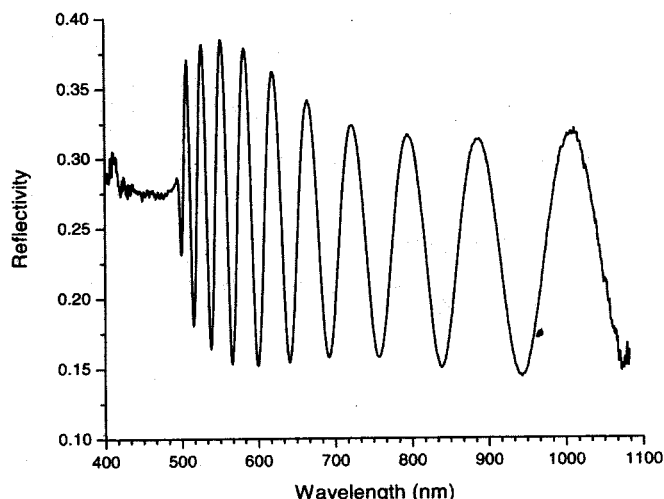


Fig. 2. A room-temperature reflectivity spectrum obtained for $\text{Zn}_{0.831}\text{Be}_{0.169}\text{Te}$.

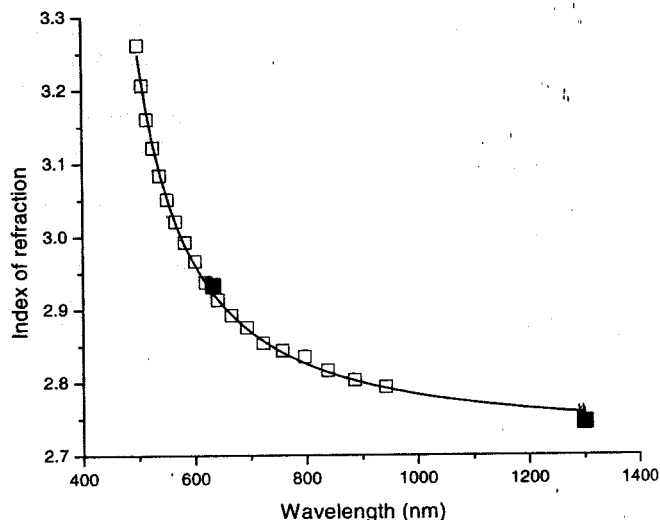


Fig. 3. The dispersion of the index of refraction of $\text{Zn}_{0.831}\text{Be}_{0.169}\text{Te}$ obtained by the prism-coupler (full squares) and the room-temperature reflectivity (open squares) techniques. The solid line corresponds to a Sellmeier-type dispersion fit obtained for the experimental data.

rays that are reflected from the air/film and from the film/substrate interfaces. As mentioned before, by using the two n values (i.e., at 632.8 nm and 1300 nm) as well as the thicknesses obtained from the prism-coupler technique, one can determine the n values corresponding to each of the extrema in the reflection spectrum. Figure 3 displays the dispersion of n obtained for $\text{Be}_x\text{Zn}_{1-x}\text{Te}$ using both the prism-coupler data (full squares) and the reflectivity data (open squares). The solid line displayed in the figure corresponds to a Sellmeier-type dispersion fit obtained for the experimental data.¹² As can be seen in Fig. 3, the increase of n as the wavelength decreases reflects the dispersion expected as the photon energy of light approaches the fundamental energy gap of the $\text{Be}_x\text{Zn}_{1-x}\text{Te}$ alloy.

ELLIPSOMETRIC RESULTS

Spectroscopic ellipsometry is a nondestructive optical-characterization technique that gives information on dielectric functions, band-structure critical points, thickness, interfaces, as well as the semiconductor-alloy composition. Compared to the prism coupler and the reflectivity technique described previously, it has the distinct advantage of obtaining n both below and above the fundamental absorption edge of the semiconductor system. However, the ellipsometric measurement is an indirect method to obtain the dielectric response of a multilayer structure, whereby one has to simulate a layered model (with a varying thickness and a dielectric function for each layer in the model) until a proper theoretical fit is obtained that accurately describes the experimental spectra.⁷ It is, therefore, advantageous to know some of the parameters of the structure a priori in order to increase the reliability of the values obtained for the dielectric function of the semiconductor layer by such modeling. In this work,

the prism coupler and the reflectivity results obtained prior to performing the ellipsometric method will serve this function.

The spectroscopic analysis was performed using an ellipsometer, capable of taking ellipsometric data with photon energies of 0.7–6.5 eV. For each sample, we obtained room-temperature ellipsometric data at angles of incidence of 65°, 70°, and 75°. The two parameters, ψ and Δ , measured by ellipsometry at each wavelength are related to the ratio of reflection coefficients by

$$\rho = R_p/R_s = \tan(\psi)e^{i\Delta}$$

where R_p is the complex-reflection coefficient for light polarized parallel to the plane of incidence, and R_s is the coefficient for light polarized perpendicular to the plane of incidence. Here, both ψ and Δ are presented in terms of two angles that are a function of both wavelength and the angle of incidence. In Fig. 4, we show the ψ and Δ spectra for the $\text{Zn}_{0.831}\text{Be}_{0.169}\text{Te}$ alloy sample obtained from the ellipsometer. In the ψ spectrum (Fig. 4a), the observed oscillations at the higher wavelength range are due to Fabry-Perot interference within the $\text{Zn}_{1-x}\text{Be}_x\text{Te}$ film. The film is both transparent and below its energy gap in the spectral range where these oscillations occur. As one observes in Fig. 4a, the disappearance of the oscillations around 480 nm signals the transition from the transparent region to the absorption region in the semiconductor.

For a given specimen, the ψ and Δ obtained from the ellipsometric measurement depend on the optical properties of the entire structure. For the alloys used in this study, a four-layer model (i.e., InP substrate, InGaAs buffer, $\text{Zn}_{1-x}\text{Be}_x\text{Te}$ layer, and surface-oxide layer) was constructed for each sample. The optical constants of the modeled oxide layer were an average between that of air and the $\text{Zn}_{1-x}\text{Be}_x\text{Te}$ layer beneath. It must be mentioned that the optical properties of the substrate and the buffer are already

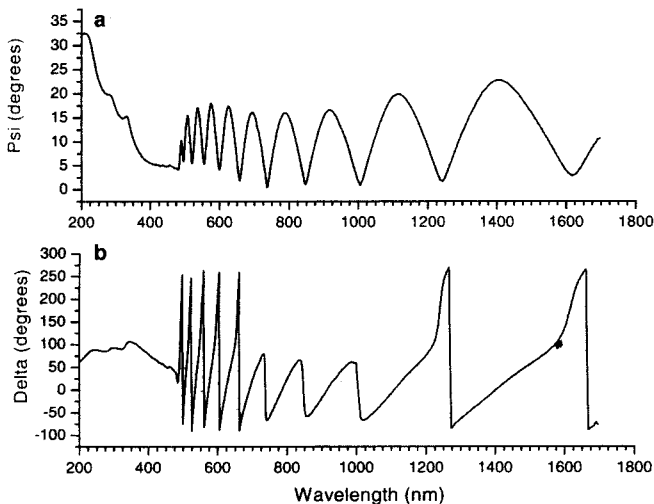


Fig. 4. The (a) ψ and (b) Δ spectra of $\text{Zn}_{0.831}\text{Be}_{0.169}\text{Te}$ measured by spectroscopic ellipsometry for an angle of incidence of 75°.

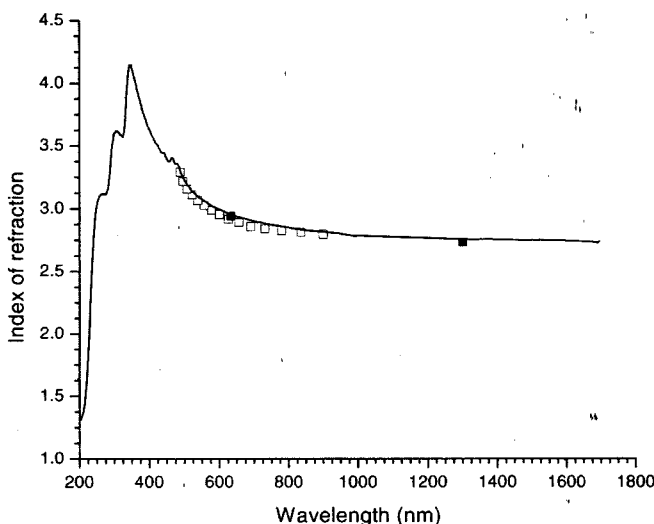


Fig. 5. The dispersion of the index of refraction of $\text{Zn}_{0.831}\text{Be}_{0.169}\text{Te}$ determined by ellipsometry (solid line), reflectivity (open squares), and prism-coupler (filled squares) techniques.

known.¹³ Hence, the parameters that need to be varied in the model are the thicknesses of each layer and the dielectric constant of the $\text{Zn}_{1-x}\text{Be}_x\text{Te}$ layer. However, because we already know the thickness of the $\text{Zn}_{1-x}\text{Be}_x\text{Te}$ layer as well as its dispersion of n below the energy gap from our previous prism-coupler and reflectivity measurements, the ellipsometric analysis will be further simplified.

The n determined from this procedure is plotted in Fig. 5 for the same $\text{Zn}_{1-x}\text{Be}_x\text{Te}$ sample as in Figs. 1 and 2. In Fig. 5, both the prism-coupler and the reflectivity data are also plotted as filled squares and open squares, respectively. We see in this case that the prism-coupler and the reflectivity data stand to guide the ellipsometric data. The excellent agreement in the data obtained below the fundamental gap from all three experimental methods gives credence to the above-bandgap dispersion of n determined by ellipsometry. In observing the ellipsometric spectra obtained for the different $\text{Zn}_{1-x}\text{Be}_x\text{Te}$ samples, we immediately notice that the incorporation of Be into the lattice blue shifts the energy gap in the $\text{Zn}_{1-x}\text{Be}_x\text{Te}$ -alloy system. In addition, we also observe the presence of distinct excitonic peaks in the dielectric spectra of samples with higher Be concentration, which also indicates the high crystalline structure of the $\text{Zn}_{1-x}\text{Be}_x\text{Te}$ alloy used for this study.

In measuring ψ and Δ of the $\text{Zn}_{1-x}\text{Be}_x\text{Te}$ alloy samples, we did not use chemical-etching procedures to eliminate $\text{Zn}_{1-x}\text{Be}_x\text{Te}$ -surface oxide that could influence the ellipsometric results.¹⁴ However, by adding a surface-oxide layer to our semiconductor model, we were able to circumvent the need for such surface treatments.¹⁵ Additionally, it must also be mentioned that the thin films used in this study were relaxed as their thicknesses exceeded the critical thickness for strain relaxation.¹⁶ Hence, we expect that the dispersion of n calculated for our thin films of $\text{Zn}_{1-x}\text{Be}_x\text{Te}$ to be essentially that of bulk $\text{Zn}_{1-x}\text{Be}_x\text{Te}$.

CONCLUSIONS

In summary, we have used a combination of prism coupler, reflectivity, and spectroscopic ellipsometry to measure the index of refraction of a series of MBE-grown $Zn_{1-x}Be_xTe$ alloys. The discrete values of n as well as the film thickness obtained from the prism coupler are used to analyze the reflectivity spectra and to obtain n as a function of wavelength. These two experimental methods allow one to find the dispersion of n for a film below its fundamental energy gap. By using the data obtained from these two methods as input parameters in analyzing the ellipsometric spectra, one can obtain the dispersion of n for the $Zn_{1-x}Be_xTe$ -alloy system at wavelengths above its fundamental energy gap. Hence, by combining the techniques of prism coupler, reflection spectroscopy, and ellipsometry, one is able to accurately determine the dispersion of n for a semiconductor thin film both below and above its fundamental energy gap.

ACKNOWLEDGEMENTS

The authors thank Professor J.K. Furdyna for allowing the use of the prism coupler in his lab. Acknowledgement is also made to the donors of the American Chemical Society Petroleum Research Fund (ACS PRF No. 38069) for support of this research.

REFERENCES

1. G. Landwehr, F. Fischer, T. Baron, T. Litz, A. Waag, K. Schull, H. Lugauer, T. Gerhard, M. Keim, and U. Lunz, *Phys. Status Solidi B* 202, 645 (1997).
2. S.B. Che, I. Nomura, W. Shinozaki, A. Kikuchi, K. Shimomura, and K. Kishino, *J. Cryst. Growth* 214, 321 (2000).
3. M.W. Cho, S.K. Hong, J.H. Chang, S. Saeki, M. Nakajima, and T. Yao, *J. Cryst. Growth* 214/215, 487 (2000).
4. O. Maksimov and M.C. Tamargo, *Appl. Phys. Lett.* 79, 782 (2001).
5. H. Okuyama, K. Nakano, T. Miyajima, and K. Akimoto, *Jpn. J. Appl. Phys.* 30, L1620 (1991).
6. F.C. Peiris, S. Lee, U. Bindley, and J.K. Furdyna, *J. Appl. Phys.* 84, 5194 (1998).
7. C.M. Herzinger, P.G. Snyder, F.G. Celii, Y.-C. Kao, D. Chow, B. Johs, and J.A. Woollam, *J. Appl. Phys.* 79, 2663 (1996).
8. O. Maksimov (Ph.D. thesis, City College and Graduate Center, CUNY, 2001).
9. P.K. Tien and R. Ulrich, *J. Opt. Soc. Am.* 60, 1325 (1970).
10. F.C. Peiris, S. Lee, U. Bindley, and J.K. Furdyna, *J. Electron. Mater.* 29, 798 (2000).
11. F.C. Peiris, S. Lee, U. Bindley, and J.K. Furdyna, *J. Appl. Phys.* 86, 918 (1999).
12. M. Born and E. Wolf, *Principles of Optics*, 3rd ed. (New York: Pergamon, 1965), p. 52.
13. C. Pickering, R.T. Carline, M.T. Emeny, N.S. Garawal, and L.K. Howard, *Appl. Phys. Lett.* 60, 2412 (1992).
14. K. Sato and S. Adachi, *J. Appl. Phys.* 73, 926 (1993).
15. H.C. Ong and R.P.H. Chang, *Appl. Phys. Lett.* 79, 3612 (2001).
16. J.W. Matthews and A.E. Blakeslee, *J. Cryst. Growth* 27, 118 (1974).